Rev.Adv.Mater.Sci. 6 (2004) 7-11

OXYGEN DIFFUSION IN NANOCRYSTALLINE ZrO_2

U. Brossmann[1], G. Knöner[2], H.-E. Schaefer[2] and R. Würschum[1]

[1]Institute of Technical Physics, Graz University of Technology, Petersgasse 16, A-8010 Graz, Austria
[2]Institute of Theoretical and Applied Physics, University of Stuttgart, D-70550 Stuttgart, Germany

Received: July 19, 2003

Abstract. Stabilized $ZrO_2 \cdot Y_2O_3$ represents one of the most promising materials for technical applications as a solid electrolyte in sensors and fuel cells, since it combines a high ionic conductivity of oxygen with mechanical and chemical resilience. The question, whether the oxygen conductivity can be further enhanced by nanostructurization, is of key importance for the development of solid oxide fuel cells (SOFC), as lower operating temperatures greatly improve the efficiency and working lifespan. The oxygen self-diffusion has been studied on highly dense, nanocrystalline specimens of both un-doped and Y_2O_3 alloyed ZrO_2 using ^{18}O as a tracer and secondary ion mass spectroscopy (SIMS). The results of tracer diffusion studies will be discussed in context of recent studies on the electric conductivity and diffusion data from literature and focusing on the role of grain boundaries.

* Presented at International Conference Nanomaterials and Nanotechnologies (Crete, Greece, August 30-September 6, 2003)

1. INTRODUCTION

Whereas comprehensive data is available on the diffusion in metals and alloys (see [1] for a review on nanostructured metals and alloys), until recently only few data have been available for ceramic materials and nanostructured oxides in particular. Nevertheless, oxide ceramics are progressively gaining importance for use as refractory structural and functional materials, e.g. for electrical and electronic applications [2]. The present review will focus on zirconium dioxide as an important model system, both with regard to technical application and basic research.

In so-called stabilized zirconia the tetragonal or cubic crystallite structure is maintained at ambient temperature by alloying with several mol.% of di- or trivalent cations as Ca^{2+}, Mg^{2+} or – most frequently – Y^{3+}. By doping with these subvalent cations, structural vacancies are introduced on the oxygen sublattice, which, on the one hand, stabilize the cubic phase at all temperatures allowing for the preparation of bulk materials and single crystals and, on the other hand, give rise to a fast ionic conduction of oxygen. With regard to technical applications in sensors and fuel cells, a key question arises, whether the introduction of a large fraction of interfaces by nanostructurization will contribute to a further enhancement of the oxygen diffusivity. Undoped ZrO_2 with a monoclinic equilibrium structure is not suitable for technical applications, as it undergoes a 7% volume shrinkage at the monoclinic-to-tetragonal phase transition at about 1100 °C. Nevertheless, it is important to study the undoped, monoclinic ZrO_2 as a model system to obtain a comprehensive picture of the diffusion behavior.

The present review on the oxygen diffusion in both un-doped and Y_2O_3-doped ZrO_2 will focus on the authors' experimental studies, where profiles of the ^{18}O tracer diffusion were being measured for the first time on nanostructured samples [3,4].

The studies confirm reports in the literature [5,6] showing a much improved sintering behavior in both Y_2O_3-doped and undoped ZrO_2. In both cases, practically fully dense ($\rho/\rho_{bulk} \geq 0.95$) specimens with a grain size in the order of 100 nm could be obtained. The powders were pre-compacted at ambient temperature applying a high pressure of 0.7 to 2 GPa

Corresponding author: U.Brossmann, e-mail: brossmann@tugraz.at

and subsequently pressure-less sintered at temperatures of about 1000 °C, which is much lower than the temperature required for fully dense sintering of coarse grained materials [3-5].

Both the improved sintering behavior and a substantial reduction in brittleness, which even allows superplastic forming of Y_2O_3 alloyed ZrO_2 at about half the melting temperature [6], are ascribed to an enhanced diffusivity induced by a large volume fraction of interfaces. In ionic conductors, the diffusion of the more mobile species, as oxygen in the case of ZrO_2, can be investigated both by the direct method of tracer techniques and by impedance spectroscopy. Assuming the electronic contribution to be negligible, the electrical conductivity σ in homogeneous ionic conductors is related to the diffusion coefficient D_i, the concentration n_i and the electric charge q_i of the ionic charge carriers according to the Nernst-Einstein relation

$$\sigma = \frac{n_i q_i^2}{kT} D_i \,. \qquad (1)$$

The ratio of the diffusion coefficient of the ionic charge carriers D_i and the tracer diffusivity D_T is known as Haven's ratio. In the case of single crystals, D_T/D_i is about 0.7 to 0.8 [7].

In the present case of nanocrystalline Y_2O_3-doped ZrO_2 (YSZ), we will summarize the data available on the enhanced oxygen diffusivities in interfaces and discuss these data together with presently availably impedance studies [5,6,8-10].

2. SYNTHESIS AND CHARACTERIZATION

In this section, the synthesis techniques and the characterization of the highly dense, nanocrystalline ZrO_2 specimen required for studying the self diffusion of oxygen, will be presented without going much into detail. A description of the measurement as well as the modeling of the electrical conduction in anionic conductors is given by H.L. Tuller [8], P. Heitjans and S. Indris [9], and X. Guo [11].

Both undoped [3] and Y_2O_3 (6.9 mol.%) alloyed [4] nanocrystalline ZrO_2 specimens have been prepared by DC magnetron sputtering of pure Zr or $Zr_{84}Y_{16}$ alloy targets and crystallite condensation in an Ar atmosphere of about 200 Pa, subsequent slow oxidation and in-situ uni-axial compaction. Applying a high pressure of 2 GPa, disk-shaped specimen (5 or 8 mm in diameter) with green densities of more than 80% were obtained. In the case of the Y_2O_3-alloyed specimen, x-ray diffraction showed a tetragonal or cubic structure with a mean crystallite size of less than 5 nm. Before annealing, the undoped n-ZrO_2 specimens similarly consisted mainly of small tetragonal grains (d < 5nm). A minor fraction of larger (10-15 nm) monoclinic grains was also observed in some of the undoped ZrO_2 specimen together with traces of un-oxidized Zr metal. Annealing in pure oxygen lead to a complete oxidation, densification, grain growth and, in the case of the undoped n-ZrO_2, to a complete transformation to the monoclinic phase. After pressure-less sintering at temperatures in the range of 970 to 1080 °C, the specimens had a mass density close to the bulk value (ρ/ρ_0: 0.96 – 0.98) as determined by Archimedes' method. The mean crystallite size was in the range of 100 nm, as determined by x-ray diffraction (XRD) and transmission electron microscopy (TEM) studies. Optical and scanning electron (SEM) micrographs showed a few microcracks and residual pores between dense agglomerates of nanocrystals with a diameter of about 100 µm. The presence of micro-cracks may give rise to an increased background level of ^{18}O ranging from 0.2% to several %, as described below.

3. DIFFUSION

The diffusion anneals were carried out in an atmosphere of 10^4 Pa of 95% enriched ^{18}O at temperatures ranging from 200 °C to 500 °C for the Y_2O_3 alloyed specimen and from 450 °C to 900 °C for the undoped, monoclinic ZrO_2. The ^{18}O penetration profiles were measured using the SIMS facility at Chalmers University, Gothenburg. Prior to the diffusion anneals, the n-ZrO_2 specimens were polished with diamond paste to a mean surface roughness of less than 10 nm over an area of 100x100 µm. In the SIMS analysis of the ^{18}O tracer concentration, data was collected only from the central part of a 250 x 250 µm^2 sized area sputtered with a Cs^+ beam to avoid a distorting influence of the crater walls. A mechanical profilometer was used to measure the crater depth, and thereby calibrating the diffusion profiles.

In case of the undoped, fully monoclinic n-ZrO_2 specimen, ^{18}O tracer diffusion studies covered a wide scope of temperatures and annealing times corresponding to penetration depths ranging from about 0.1 µm at 500 °C (t_a =1 h) to 10 µm at 800 °C. While the high number of interfaces allowed a detailed study of the interface diffusion based on the ^{18}O distribution at larger penetration, the diffusion in the crystallite volume could also be assessed from the initial part of the diffusion profiles, as the crystallite

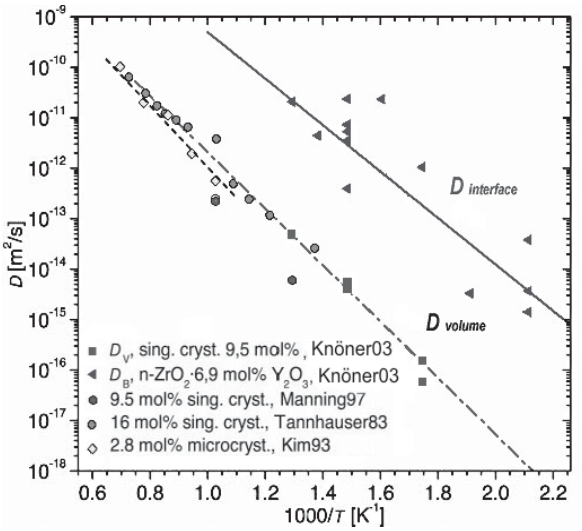

Fig. 1. Oxygen diffusivity in the interfaces of nanocrystalline Y_2O_3 (6.9 mol.%) alloyed ZrO_2 (□) and in single crystals (■) of Y_2O_3(9.5 mol.%) alloyed ZrO_2. Data from literature of single crystals or microcrystalline YSZ is shown for comparison (Adapted from [4]). © 2003 National Academy of Sciences, USA.

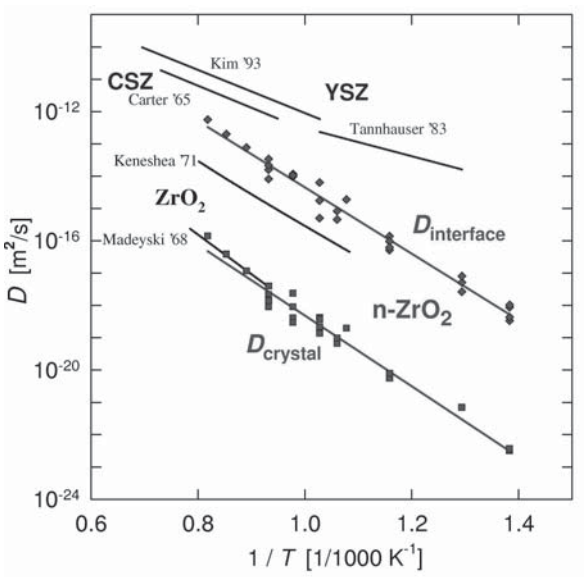

Fig. 2. Oxygen diffusivity at interfaces (◆) and the crystallite volume (■) of un-doped, nanocrystalline ZrO_2. The bulk diffusivity in CaO and Y_2O_3 alloyed ZrO_2 is shown for comparison (Adapted from [3]).

diameter *d* of 80 – 300 nm exceeds the grain boundary width (δ~0.5 nm) by a factor of 150 to 500. A detailed analysis of the ^{18}O diffusion profiles on the basis of type B diffusion kinetics [3] showed the oxygen diffusivity in interfaces to be 3 – 4 orders higher than in the volume of the pure ZrO_2 nanocrystallites. Activation energies and pre-exponential factors of Q_V = (2.29±0.1) eV, $D_{0,V}^{typeB}$ = (2.5 ± 1.5)·10^{-7} m^2/s for diffusion in the volume of the crystallites and Q_{GB}= (1.95±0.05) eV, $D_{0,GB}^{typeB}$ = (3.3 ± 1.5)·10^{-5} m^2/s for diffusion in the grain boundaries of undoped, nanocrystalline monoclinic ZrO_2 have been determined. These results for un-doped n-ZrO_2 are similar to values of the activation energies and effective diffusion coefficients reported in earlier studies on conventional polycrystalline samples [12,13].

The ^{18}O diffusion profiles in n-ZrO_2·6.9 mol.% Y_2O_3 [4] show a much deeper penetration than in single crystalline ZrO_2·9.5 mol.% Y_2O_3. For single crystals, the ^{18}O diffusion data, which have been recently extended to low temperatures [14] yield an activation energy of Q_V = (1.11 ± 0.06) eV with a pre-exponential factor of $D_{0,V}$ = 0.8·10^{-6} m^2/s and fit well to earlier data (Fig. 2).

For the analysis of the ^{18}O diffusion data in n-ZrO_2·6.9 mol.% Y_2O_3 type A kinetic of grain boundary diffusion [15] is applied making use of the single crystal data. This analysis yields an enhancement of the ^{18}O diffusivity in the interfaces of n-ZrO_3·6.9 mol.% Y_2O_3 by more than three orders of magnitude compared to the ^{18}O diffusivity in the single crystals. From the temperature variation of the interfacial ^{18}O diffusivity in n-ZrO_2·6.9 mol.% Y_2O_3 the activation enthalpy H_{GB} = 0.91 eV and the pre-exponential factor $D_{0,GB}$ = 2·10^{-5} m^2/s can be derived.

A comparison of the oxygen self diffusion in undoped and Y_2O_3(6.9 mol.%) alloyed, nanocrystalline ZrO_2 with data from literature shows, that in un-doped n-ZrO_2 both D_V and D_{GB} are significantly lower than found in the present study on n-YSZ and reported in the literature for single and poly-crystalline Y-or Ca-doped ZrO_2 (see Fig. 1, [16-18]).

The activation energies of the oxygen diffusion in undoped n-ZrO_2 of about 2 eV are significantly higher than the corresponding values in the order of 1 eV found in our recent study on Y_2O_3 doped ZrO_2 (YSZ) and single crystals [4,14] and reported in literature for CaO or Y_2O_3-alloyed ZrO_2 [17,19], which indicates a different mechanism of diffusion.

The higher activation energies found for the ^{18}O diffusion in undoped n-ZrO_2 [3] are presumably due to thermally activated migration as well as formation of oxygen vacancies. In contrast to that, the low activation enthalpy and the high diffusivity of oxygen observed in Y_2O_3 doped ZrO_2 [17,18] is fully determined by the migration of dopant-induced vacancies.

In both cases of undoped ZrO_2 [3] and of Y_2O_3 doped ZrO_2 [4], residual pores and microcracks stemming from powder agglomeration lead to an increased ^{18}O background after the diffusion anneals in comparison to the natural abundance of 0.2%, but are not presumed to affect the diffusion properties determined at higher ^{18}O concentrations.

4. CONDUCTIVITY

Turning now to studies of the DC electric conductivity or AC impedance spectroscopy, a first glance shows, that the activation energies of the electrical conductivity and the oxygen self diffusion in YSZ are both in the range of 1 eV. A detailed comparison, however, shows the behavior of the electrical conductivity in polycrystalline YSZ to differ substantially from tracer diffusion, which is significantly enhanced at interfaces with an activation energy of 0.9 eV as compared to a value of 1.1 eV in the crystallite volume (see Sect. 3). Nearly all studies on both conventional and nanostructured Y_2O_3 alloyed ZrO_2 show, that the electrical conductivity in grain boundaries is 2–3 orders of magnitude smaller than in the crystallite volume. Correspondingly, the activation energy of the electrical conduction at interfaces with values in the range of 1.0 to 1.2 eV is significantly higher than the values of 0.84 –0.93 eV observed for the bulk conductivity [5, 8].

In this respect, the studies of Kosacki *et al.* [20] on nanocrystalline thin films of Y(16%)SZ on a sapphire substrate constitute a remarkable exception, in showing both an enhanced conductivity and a lower activation enthalpy in nanocrystalline films (d_{grain} ~ 20 nm) than in coarse-grained polycrystals.

Reports in the literature show, that the observation of a reduced electrical conductivity at interfaces, which is also referred to as grain boundary blocking, is not limited to YSZ, but also observed on other oxides with a fluorite structure, as CeO_2 [14]. It is ascribed, on the one hand, to a segregation of poorly conducting silicate impurities at grain boundaries [21, 22]. In this context, clean boundaries in YSZ were expected to be highly conductive [8]. Indeed, experimental studies on fully dense, highly pure specimens of nano- and micro-crystalline CaO or Y_2O_3 alloyed ZrO_2 [5,8,11] show a significant increase of the conductivity at interfaces with decreasing crystallite size down to nm size. However, the grain boundary conductivity remained always lower than the bulk value, even where no significant amount of silica-covered interfaces was observed, indicating an intrinsic effect.

The grain boundary blocking in YSZ is therefore, on the other hand, also ascribed to the formation of electric space charge layers at interfaces, as supported by several more recent studies. Electrochemical and theoretical studies by Guo and Maier [10] on microcrystalline ZrO_2 alloyed with 2 to 8 mol.% Y_2O_3 indicate the presence of an approx. 5 nm wide, poorly conducting layer at interfaces. Both analytic studies by means of HRTEM and EELS and atomistic modeling show a significant segregation of Y^{3+} to the GBs and a depletion of Y^{3+} in the adjoining grains [9-11,23,24]. At the GB cores (δ~0.8 nm), the high density of vacant oxygen lattice sites contributes to a positive space charge and a noticeable concentration of free electrons. In the adjoining Y^{3+} depleted zones, a negative space charge and a very low concentration of oxygen vacancies prevails on the length scale corresponding to the Debye length of a few nm, which contributes to forming a Schottky barrier [10,11,23,24]. The space charge model is supported by the segregation behavior of dopant cations, as the tri-valent Al segregates strongly forming Al_2O_3 particles at interfaces, while the penta-valent Nb as an electron donor does not [25,26].

In the framework of the Nernst-Einstein model (Eq.(1)) of the ionic conduction in solids [7], the results of the presently available tracer diffusion [3,4] and electric impedance studies [5,8,10] appear to be not compatible. However, it is not clear, whether this simple relation referring to homogeneous media is applicable to heterogeneous materials and grain boundaries. In nanocrystalline materials, the diffusion and electrical conduction behavior within the large volume of interfaces may also differ substantially from bulk properties. In addition, specimens prepared via powders routes may contain small amounts of residual pores and microcracks, which may have substantial diametrical influence providing – at the same time – pathways of rapid diffusion and obstacles to the electrical conductivity by reducing the contacting interface area.

A comprehensive assessment of the diffusion and electrical conductivity in ZrO_2 therefore requires further studies on fully dense, well-defined specimens made from high purity components. Ideally, tracer diffusion and electrical impedance measurements should be carried out on identically prepared samples.

REFERENCES

[1] R. Würschum, S. Herth, and U. Brossmann // *Adv. Eng. Mater.* **5** (2003) 365.

[2] N. Setter and R. Waser // *Acta mater.* **48** (2000) 151.
[3] U. Brossmann, R. Würschum and U. Södervall // *J. Appl. Phys.* **85** (1999) 7646.
[4] G. Knöner, K. Reimann, R. Röwer and H.E. Schaefer // *PNAS* **100** (2003) 3870.
[5] P. Mondal, A. Klein, W. Jaegermann and H. Hahn // *Solid State Ionics* **118** (1999) 331.
[6] U. Betz, K.H. Padmanabhan and H. Hahn // *J. Mater. Sci* **36** (2001) 5811.
[7] *Impedance Spectroscopy*, ed. by J.R. McDonald (J. Wiley & Sons, 1983).
[8] H.L. Tuller // *Solid State Ionics* **131** (2000) 143.
[9] P. Heitjans and S. Indris // *J. Phys: Condens. Matter* **15** (2003) 1257.
[10] X. Guo and J. Maier // *J. Electrochem. Soc.* **148** (2001) 121.
[11] X. Guo // *Computational Materials Science* **20** (2001) 168.
[12] A. Madeyski and W.W. Smeltzer // *Mater. Res. Bull.* **3** (1968) 369.
[13] F.J. Keneshea and D.L. Douglas // *Oxidation of metals* **3** (1971) 1.
[14] R. Röwer, G. Knöner, K. Reimann, H.-E. Schaefer and U. Södervall // *phys. stat. Sol (b)* **239** (2003) R1.
[15] I. Kaur, Y. Mishin and W. Gust, *Fundamentals of Grain and Interphase Boundary Diffusion* (J. Wiley & Sons, Chichester, UK 1995).
[16] L.A. Simpson and R.E. Carter // *J. Amer. Ceram. Soc* **76** (1966) 139.
[17] D.S. Tannhauser, J.A. Kilner and B.C.H. Steele // *Nucl. Instrum. Methods* **281** (1983) 504.
[18] B.K. Kim, S.J. Park and H. Hamaguchi // *J. Am. Ceram. Soc.* **76** (1993) 2119.
[19] P.S. Manning, J.D. Sirman, R.A. Souza and J.A. Kilner // *Solid State Ionics* **100** (1997) 1.
[20] I. Kosacki, B. Gorman and H.U. Anderson, In: *Ionic and Mixed Conductors Vol. III,* ed. by T.A. Ramanarayanam *et al.* (Electrochemical Society, Pennington, NJ, 1998) p. 631.
[21] S.P.S. Badwal // *Solid State Ionics* **76** (1995) 67.
[22] M. Aoki, Y-M. Chiang, I. Kosacki, J.-R. Lee, H.L. Tuller and Y.J. Liu // *J. Amer. Ceram. Soc.* **69** (1996) 1169.
[23] Y. Lei, Y. Ito and N.D. Browning // *J. Am. Ceram. Soc.* **85** (2002) 2359.
[24] E.C. Dickey, X. Fan and S.J. Pennycook // *J. Am. Ceram. Soc.* **84** (2001) 1361
[25] X. Guo // *Solid State Ionics* **96** (1997) 247.
[26] X. Guo // *Solid State Ionics* **99** (1997) 137.